ELSEVIER

Biochimica et Biophysica Acta 1460 (2000) 166–176

BIOCHIMICA ET BIOPHYSICA ACTA
BBA

www.elsevier.com/locate/bba

Review

Structures of photointermediates and their implications for the proton pump mechanism

Mikio Kataoka [a,*], Hironari Kamikubo [b]

[a] *Department of Materials Science, Nara Institute of Science and Technology, 8916-5, Takayama-machi, Ikoma, Nara 630-0101, Japan*
[b] *Institute of Materials Structure Science, High Energy Accelerator Research Organization, Tsukuba, Ibaraki 350-0801, Japan*

Received 24 March 2000; accepted 24 March 2000

Abstract

It is widely accepted that bacteriorhodopsin undergoes global conformational changes during its photocycle. In this review, the structural properties of the M and N intermediates are described in detail. Based on the clarified global conformational change, we propose a model for the molecular mechanism of the proton pump. The global structural change is suggested to be a key component in establishing vectorial proton transport.

Keywords: Bacteriorhodopsin; Structure of photointermediate; X-Ray diffraction; Proton pump mechanism; Light-induced conformational change

1. Introduction

The elucidation of the molecular mechanism of protein function based on the tertiary structure is one of the essential issues in modern biological science. The elementary processes of protein function are chemical reactions at the amino acid residue level, such as ligand binding, protonation/deprotonation of dissociable residues and so on. The global structure should control these local chemical reactions and their orders. For the understanding of protein function, it is necessary to reveal the intramolecular local changes at amino acid residue level and the global structural changes over the whole molecule during the reaction process, and the interrelationship between these changes. From the standpoint of this view, we deal with bacteriorhodopsin (bR), a light-driven proton pump, as a model system for the elucidation of protein function. In any active transport system, the access of the transported ion at the active site changes from one membrane side to the other during the reaction. Thus, it is expected that the global conformational change is related closely to the local changes. In this review, we focus on the structures of some photointermediates of bR and the role of the conformation change on the proton pump mechanism.

bR forms a two-dimensional crystal in the cell membrane of *Halobacterium salinarum*, called the 'purple membrane' [1]. Utilizing this exceptional property, diffraction techniques have been applied to reveal its structure. The tertiary structure was first solved by electron diffraction and microscopy to 3 Å resolution [2–5]. The detailed structure to 1.5 Å res-

* Corresponding author. Fax: +81 (743) 726109; E-mail: kataoka@ms.aist-nara.ac.jp

0005-2728/00/$ – see front matter
PII: S0005-2728(00)00137-7

olution is determined by X-ray crystal structural analysis [6–8]. bR is composed of seven transmembrane α-helices (named A to G from the N terminus) with short interconnecting loops (Fig. 1). The chromophore, retinal, is covalently bound to Lys216 in the G helix via protonated Schiff base [9]. The retinal is buried in the central part of the protein, as shown in Fig. 1.

Absorption of a photon by the retinal triggers a series of reactions that bring about vectorial proton transport, from cytoplasm to the outside of the cell. The photointermediates are termed J, K, L, M, N, and O, which are characterized by their absorption spectra (for a review, see [10,11]). Proton uptake from the cytoplasmic side occurs after N formation, while proton release to the extracellular space is an event at the time of M formation. Structural information on these intermediates is crucial to understand the proton pump mechanism. Several groups observed large conformational changes at the M and the N intermediates, by X-ray, neutron and electron diffraction [12–17]. On the other hand, chemical reactions at amino acid residue level characteristic to each photointermediate are revealed by spectroscopic measurements [11,18,19] and the proton pathway is assigned in the tertiary structure (Fig. 1).

The important question remaining is how the vectorial proton transport is controlled, that is, how back reaction is suppressed during the photocycle. Below we call the mechanism 'reprotonation switch' or 'switch'. We consider that protein should undergo global structural changes during a series of chemical reactions at the amino acid residue level. In the case of bR, a proton is first transferred from the Schiff base to Asp85 located in the extracellular channel at a distance of 4 Å from the Schiff base. The Schiff base then reprotonates from Asp96 in the opposite side. The global conformational changes at the M and N intermediates revealed so far [12–17] should be an essential component of the switch mechanism [20,21]. In this review, we summarize the structures of the M and N intermediates and the possible structural transition between M and N. We will propose a model for the proton pump based on the global conformational changes and the relationship between the global structure, and the local chemical reactions characteristic to each intermediate.

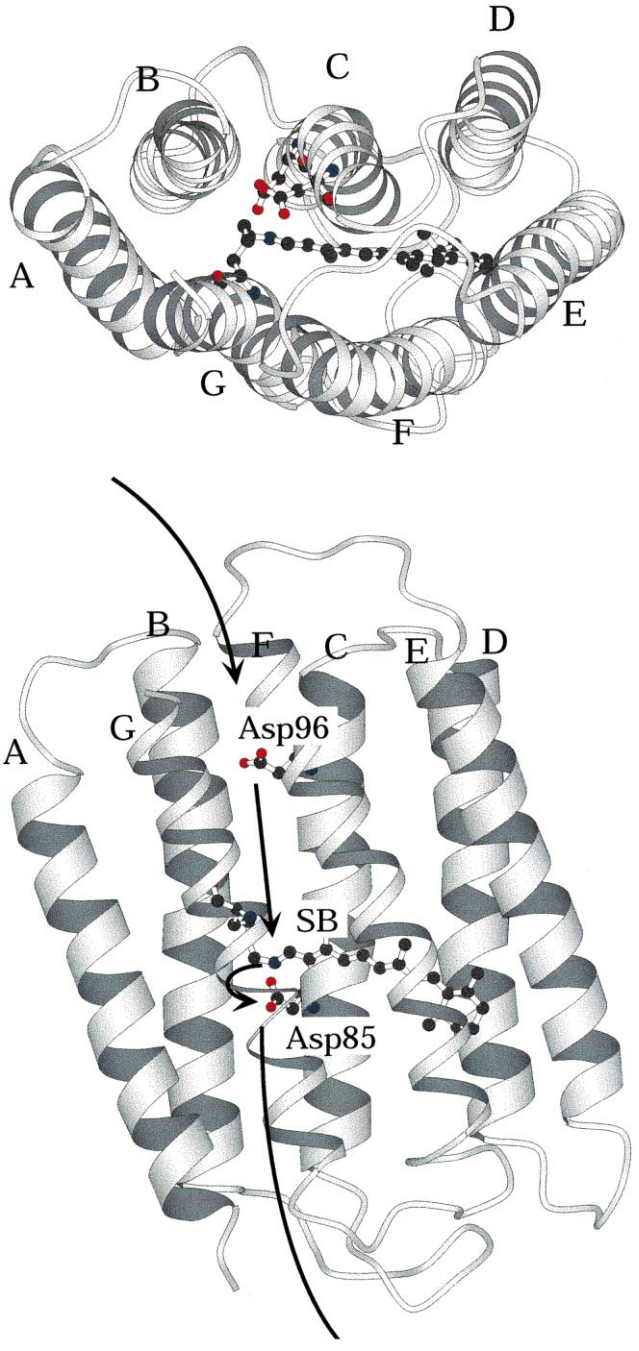

→

Fig. 1. Tertiary structure of bacteriorhodopsin revealed by electron microscopy and image reconstruction method [3]. The several amino acid residues participating in the proton pump are superimposed on the structure. The figure was drawn with MOLSCRIPT [39].

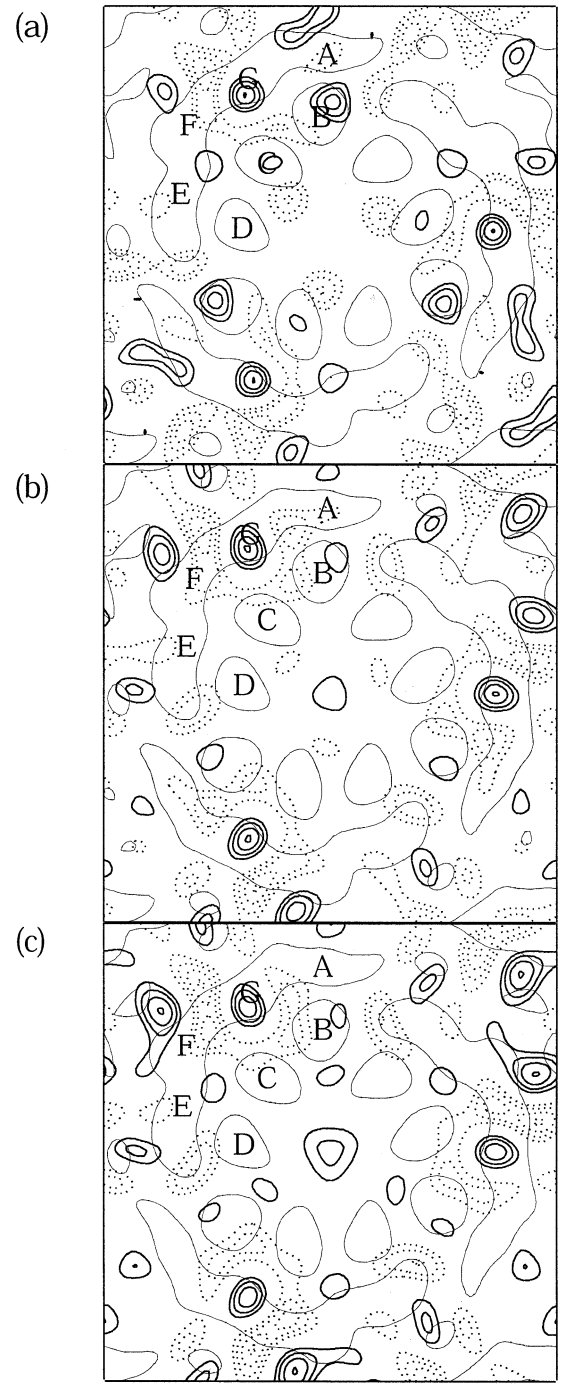

Fig. 2. Two-dimensional difference electron density maps between the intermediate state and the dark state. (a) M intermediate for arginine treated wild type bR; (b) M intermediate for D96N mutant bR under alkaline condition; (c) N intermediate for F171C mutant bR.

→

2. Tertiary structural changes during the photocycle of bR

2.1. Structure of the M intermediate

To reveal the structure of a photointermediate by diffraction techniques, it is necessary to accumulate the specific intermediate in sufficient amounts during the diffraction measurements. Some procedures, including trapping at low temperature, chemical treatment and the utilization of mutant bR, have been successfully applied to the structural studies of photointermediates. It is now widely accepted that bR undergoes a global conformational change upon light absorption [12–17,22,23]. The change is observed around helices B, F and G (Fig. 2). This is in contrast with the earliest work on the M intermediate which demonstrated that no essential structural changes occurred, even though the sample was composed of pure M intermediate [24]. This apparent discrepancy is explained by the fact that the earlier sample has insufficient hydration, while the other samples are sufficiently hydrated [15]. The hydration dependent global conformational change is confirmed by Sass et al., who observed no global conformational change below 57% relative humidity with complete deprotonation of Schiff base, but detected global conformational change above 57% relative humidity [25]. The former corresponds to the M_1 state and the latter to the M_2 state. Global conformational change was suggested to occur during the M_1 to M_2 transition. Inelastic neutron scattering studies gave a physical explanation for the M_1 to M_2 transition [26]. The dehydrated bR shows only harmonic motion between very low temperature and room temperature, while sufficiently hydrated bR shows a so-called glass transition. At very low temperature, the allowed motions are only harmonic vibrations, but above the glass transition temperature (180–200 K) the hydrated bR shows anharmonic motions. Complete photocycle is observed only for hydrated bR and only above the glass transition temperature [26]. Therefore, anharmonic motions of the protein are required to activate the conformational change [26,27]. The M_1 to M_2 transition and its physical explanation bring two important conclusions for the proton pump mechanism. One is that the first local chemical reaction at amino acid residue

level (proton transfer from Schiff base to Asp85) can proceed without any global conformational change and without hydration or below glass transition temperature. The other is that the global conformational change is required to complete photocycle and proton translocation. It is also suggested that the local chemical reaction induces the global conformational change.

The major changes at the M_2 intermediate are observed around helices B, F and G. However, there are small but significant differences among the structures reported so far. Dencher et al. examined the structure of the M intermediate by neutron diffraction [12]. The M intermediate was accumulated by guanidinium HCl at alkaline pH. The sample composed of the pure M intermediate was then cooled down to 93 K to trap the intermediate during neutron exposure. The overall relative change defined as $\Sigma|\Delta I|/\Sigma I$ (we call it *R*-factor hereafter) is about 9%. The calculated difference electron density map shows the major changes around helices G and F with a minor change around helix B [12]. The measurement of diffraction at very low temperature brings shrinkage of the lattice constant from 62.5 Å to 61.3 Å [28]. Further, they observed a small increase of the lattice constant (0.3 Å) after the formation of the M intermediate [12]. These are disadvantages for structural analysis. However, similar structural changes to their result were observed by Koch et al. [13] using D96N mutant bR with X-ray diffraction. The *R*-factor was about 9%. The lattice constant increased by 0.3 Å. Fig. 2b shows the difference density map of D96N. The narrow line represents the bR molecule. The average electron density of the M intermediate increases at the region represented by a bold line, and decreases at the region represented by a dotted line. Major changes around helices F and G, with a minor change around helix B, are clearly observed.

We found that arginine treatment of wild type bR prolongs the lifetime of the M intermediate at room temperature [29]. We carried out X-ray diffraction experiments on the arginine-treated wild type bR in the presence and the absence of continuous illumination at room temperature, and observed distinct changes in diffraction profiles [14]. The *R*-factor is 6.9%, which is smaller than the results introduced above. The lattice constant of the dark state was 62.81 Å and that of the M intermediate was 62.95 Å. The increase is smaller than the results introduced above. The difference electron density map calculated from the intensity changes is shown in Fig. 2a. Significant changes are found around the B and G helices, with only a minor change around helix F. We consider that the differences between Fig. 2a and b are small but significant. These two types of structural changes were also observed with electron microscopy and diffraction [15].

Subramaniam et al. trapped the M intermediate by flash-freezing after triggering the photoreaction by pulse excitation [15]. They could observe the structure of wild type intermediate under a near physiological condition without any chemical treatment by electron diffraction. They also carried out the same experiments with D96G mutant bR. The replacement of the residue prolongs the life of the M intermediate as is in the case of D96N. The structural changes observed for the wild type are similar to our difference electron density map (Fig. 2a), and those for D96G to the maps by Dencher et al. [12] and Koch et al. [13] (Fig. 2b). In their interpretation, the differences in the structure of the intermediates of wild type and D96G are due to the different composition of the trapped state, because their method traps a mixture of intermediates. Based on the estimation that the wild type sample consists of 63% M intermediate and 26% N intermediate, they explained that the feature of the N intermediate appears in their map of the wild type [15]. On the other hand, FTIR studies of D96N under the same condition as that used by Koch et al. [13] indicated that although both infrared and visible spectra indicated that only the M intermediate was present (deprotonated Schiff base), the protein had structural properties in the N intermediate exclusively [30]. The structure of the N intermediate was required for the further understanding of the photocycle and proton pump mechanism.

2.2. Structure of the N intermediate

The F171C mutant bR accumulates exclusively the N intermediate at neutral pH under continuous illumination. Thus, we succeeded in measuring the protein structural change in the N intermediate [16]. The difference electron density map shown in Fig. 2c clearly indicates that marked changes occur around helices G and F. A characteristic pair of positive and

negative peaks can be seen around the F helix. These properties are similar to the results obtained for the M intermediate of D96N by Dencher et al. [12] and Koch et al. [13]. The correlation coefficient of the structural changes between F171C and D96N is more than 0.90, indicating that the two sets of data are almost identical. On the other hand, the correlation coefficient of the structural changes between F171C and arginine treated wild type is 0.83 and that between D96N and wild type is 0.70. Therefore the structure of N obtained for F171C is closer to the M intermediate of D96N than the M of the wild type [16]. The *R*-factor of the intensity changes for the N intermediate was 7%, which is smaller than that for the D96N. This is partly due to the fact that the specimen is a mixture of the N and the unphotolyzed bR for F171C. Vonck also reported the structure of the N intermediate using F219L mutant bR with electron diffraction [17]. The reported difference electron density map was almost the same as our map shown in Fig. 2c. The observed N structure supports the result of the FTIR study. The photolyzed state of D96N (and presumably D96G) possesses the deprotonated Schiff base characteristic to the M intermediate, but the conformation of protein moiety is close to the N intermediate (MN intermediate). The FTIR spectrum of the photolyzed state of the arginine treated wild type is identical with that of the M intermediate of the wild type (Kamikubo and Kataoka, unpublished result). We consider that the structure shown in Fig. 2a is the structure of the true M (M_2) intermediate.

2.3. Sidedness of the structural change

The structural changes shown in Fig. 2 are projections onto the membrane plane. With X-ray or neutron diffraction of the oriented sheet of purple membrane, it is impossible to distinguish the structural change of the cytoplasmic side from the extracellular side. Electron diffraction using tilted specimens enables reconstruction of the tertiary structural image. Despite the small difference between M and N intermediates mentioned above, it is clarified that most of the structural changes are observed at the cytoplasmic half of the molecule in both cases [15,17]. It is clearly demonstrated that the pair of positive and negative peaks near F helix shown in Fig. 2 are ascribed to the tilt of the F helix in the cytoplasmic half toward outside. The movement corresponds to the opening of the cytoplasmic proton channel. Recently, the crystal structure analysis of the M (MN) intermediate of D96N has been published [23]. The changes in helices F and G are observed in the crystal structure.

Although X-ray (neutron) diffraction of the oriented sheet is a low-resolution technique, it can give a reasonable projection of structures for the photointermediates as discussed by Subramaniam et al. [15]. Both X-ray crystallography and high-resolution electron diffraction involve inherent difficulties, while X-ray diffraction is convenient to carry out under many different conditions. If we can distinguish the cytoplasmic side from the extracellular side by X-ray diffraction, it will be powerful and effective not only for the study of the photointermediate of bR but also for the structural studies of the other membrane proteins. For this purpose, we introduced cysteine substitutions to residues on the cytoplasmic side, and labeled them with mercury. Careful X-ray diffraction experiments enabled the estimation of intensity changes between the labeled and the non-labeled specimens [31]. Each difference electron density map showed only a single peak, which was assigned as the position of the labeled mercury [31]. The determined mercury position is very close to the expected position from the crystal structure. The mercury labeling method has been extended to the photointermediate [32]. Ile222 in the cytoplasmic side of helix G was replaced with cysteine. The cysteine was labeled with mercury. The movement of the mercury position can be identified in the projection map. The cytoplasmic side of helix G shifts toward helix F at the MN intermediate [32]. Thus, from the heavy atom labeling and X-ray diffraction, we can assign the positions of amino acid residues and their movements in a low-resolution projection map.

3. Structural change and proton transportation mechanism

3.1. M to N structural transition

Subtle but meaningful structural differences be-

tween the M intermediate and the N intermediate are established, as shown in Fig. 2. However, all the structural studies introduced so far have been performed with different samples, namely, with different chemical treatments and the use of different mutants. It should be clarified whether these two structures appear in a real photocycle. At least, we need to know whether a single specimen can assume these two different structures.

If the two structures are necessary components of the photocycle, they should bear some functional roles. In the dark state, Asp96 is protonated, indicating that the microenvironment of Asp96 is extremely hydrophobic. The characteristic chemical (local) reaction at the M intermediate is a proton transfer from Schiff base to Asp85. At this stage, Asp96 should still be protonated. The characteristic chemical reaction at the N intermediate is a reprotonation of Schiff base from Asp96. The change in helix F corresponds to the opening of the channel, which is characteristic to the structure of N intermediate. The changes in helix F are less prominent at the M intermediate as shown in Fig. 2. We assume that the cytoplasmic half of the proton channel should be closed at the M intermediate. If the channel opens at the M intermediate, Asp96 would release proton to cytoplasm rather than to Schiff base. The channel should be opened after forming the connectivity between the Schiff base and Asp96 which is established at the M intermediate. If these assumptions are correct, the channel is more hydrated in the N or MN intermediates than in M.

Based on this assumption, we examined the effect of hydration on the structures of M intermediates of D96N [33]. The intensity increase of the (20) reflection normalized to the decrease of the (11) reflection is larger for the M intermediate than for the N intermediate [33]. Fig. 3 shows light minus dark difference X-ray diffraction intensity profiles in the low-angle region that includes only the (11) and (20) reflections, obtained at different hydration levels. The profile was normalized to the change of the (11) reflection. It is clear that the increase of the (20) reflection becomes prominent at lower hydration levels. For the fully hydrated sample prepared by soaking, no intensity change in the (20) reflection was observed. These differences strongly indicate that the structural change in the photointermediate is hydration-dependent [33]. The *R*-factor for the highly hydrated sample was 9.5% while that of the lower hydration level was 6%. Fig. 4 shows different electron density maps for the lower hydration sample (Fig. 4a) and the higher hydration sample (Fig. 4b). The changes around helices B, F and G are observable in both maps, which are very similar to the various difference maps for the M and N intermediates re-

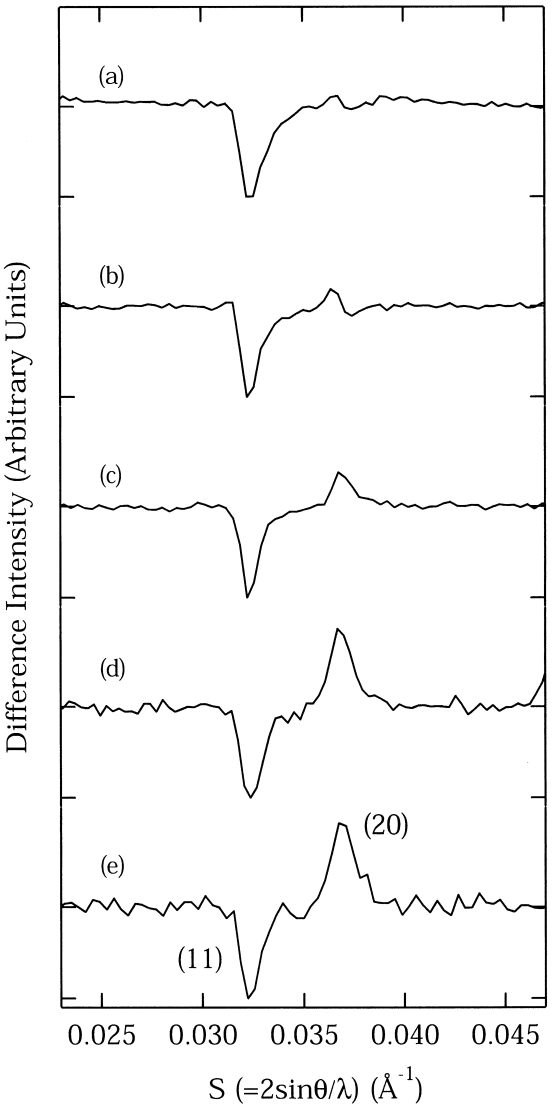

Fig. 3. Difference X-ray diffraction profiles in the low-angle region that include the (11) and (20) Bragg reflection. For comparison, the profiles are normalized by adjusting the amplitude of the (11) reflection to 1. (a) Fully hydrated sample obtained by soaking; (b) fully hydrated sample obtained by placing a drop of buffer solution for 1 h; (c) 95% relative humidity; (d) 81% relative humidity; (e) 76% relative humidity.

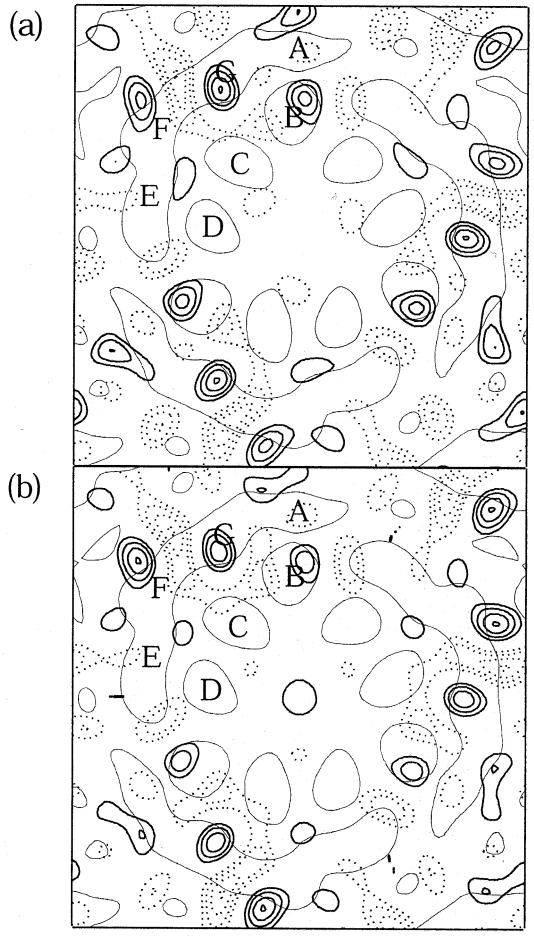

Fig. 4. Two-dimensional difference electron density maps between the M intermediate of D96N mutant bR and dark state at pH 10 (a) in a partially dehydrated sample and (b) in a hydrated sample.

ported so far and the maps shown in Fig. 2. The most prominent positive peak is near helix F in the hydrated sample, while it is the vicinity of helix B in the lower hydration sample. X-Ray diffraction strongly indicates that the observed structure is the M intermediate at the lower hydration level, while it is the MN intermediate at the higher hydration level. Difference FTIR spectra also support the conclusion of the formation of the intermediate with the M-type structure (normal M intermediate) at low humidity and of the N-type structure (the MN intermediate) at high humidity [33].

Sass et al. also reported an effect of hydration on the M intermediate for D96N [25]. They focused rather on the structural changes observed above and below 57% relative humidity. They demonstrated that a large conformational change occurs above 57% relative humidity [25]. The structural change they observed corresponds to the M_1 to M_2 transition, while we observed the M_2 to N structural transition. In their paper, the M_2 to N structural transition was not described explicitly. However, the significant changes at the B and G helices are observed in the difference electron density map obtained from the sample equilibrated at 75% relative humidity shown in their paper. On the other hand, Subramaniam et al. suggested that the structural difference between M_2 and N is trivial, if any [22]. They compared the structure obtained by quenching 1 ms after photoexcitation with that 150 ms after excitation and concluded that no significant differences in these two states were observed [22]. Their structures should be a mixture of some photointermediates, even though the content of M is more for the former than for the latter. It should be noted that the differences in diffraction appear in the same reflections for the M and the N intermediate. The comparison of the structures for the mixed photointermediates should be quite difficult. SVD analysis of the time-resolved diffraction shows that at least two different conformations exist in the photocycle of wild type bR [34]. We believe that the M_2 to N structural transition is an important component of the photocycle.

3.2. The trigger of the structural change

It is established that the global conformational change occurs during the M_1 to M_2 transition of the photocycle. At the M_1 stage, retinal isomerizes from all-*trans* to 13-*cis* and the proton is transferred from Schiff base to Asp85. It is thus required to clarify which reaction triggers the global conformational change, isomerization or deprotonation. One acceptable concept for the mechanism of an ion pump is that the association/dissociation of the transported ion to an active site of an ion pump should be closely related to the conformational change [20,21,35]. Thus, we investigated the effect of protonation/deprotonation of Schiff base on protein conformation using D85N.

Asp85 is not only the proton acceptor of the Schiff base but also the counterion stabilizing the Schiff base proton. In D85N mutant bR, the Schiff base can be deprotonated without light under alkaline

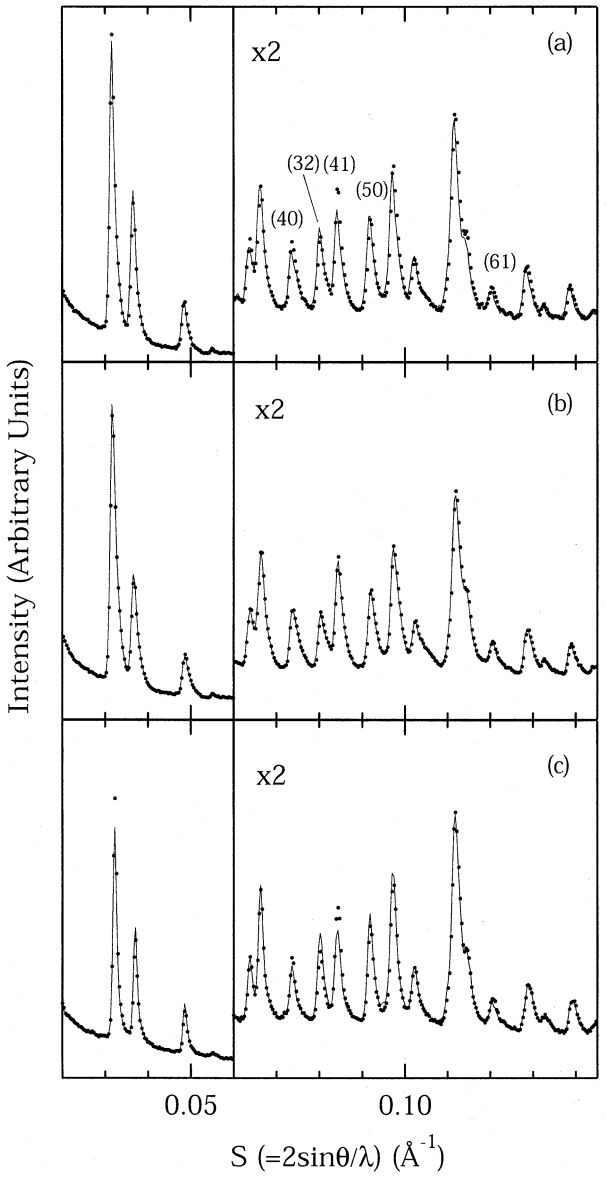

Fig. 5. X-Ray diffraction profiles of (a) D85N and (b) wild type at neutral pH (dotted line) and alkaline pH (solid line). As a reference, X-ray diffraction profiles obtained from D96N with (dotted line) and without (solid line) illumination are shown in (c).

pH. A shift of the absorption maximum from about 610 nm (blue form) to about 400 nm (yellow form) upon raising the pH from 6.0 to 10.0 is observed [36]. The absorption change upon raising the pH reflects deprotonation of Schiff base and resembles the phenomenon observed in forming the M intermediate [36]. Fig. 5a shows the X-ray diffraction intensity profiles of D85N in blue form at pH 6 (filled circles) and in yellow form at pH 11 (solid line), indicating that significant changes are generated on (40) (32) (41) reflections [20]. Fig. 5b shows the X-ray diffraction intensity profiles of wild type at pH 6 (filled circles) and pH 11 (solid line). No significant changes can be observed under the same condition as D85N. These results indicate that the protein structural changes of D85N upon changing pH is caused by the deprotonation of the Schiff base, but not by the deprotonation of amino acid residues located in the protein surface [20]. The X-ray diffraction intensity profiles obtained from the M (MN) intermediate (solid line) and the dark state bR (filled circles) using D96N are shown in Fig. 5c. Quite similar intensity changes are observed between Fig. 5a and c. The difference electron density map (Fig. 6) between the yellow and blue form of D85N indicates the structural changes around helices B, F, and G, similar to the structural changes shown in Fig. 2. We can conclude that the same type of conformational change as light-induced conformational change occurs in D85N, but without illumination [20]. Thus, we conclude that the protein structural changes in the intermediates are induced by the deprotonation of Schiff base. It is also confirmed that the deprotonation of Shiff base rather than retinal isomerization is a major cause for the conformational change using analogue retinals [37].

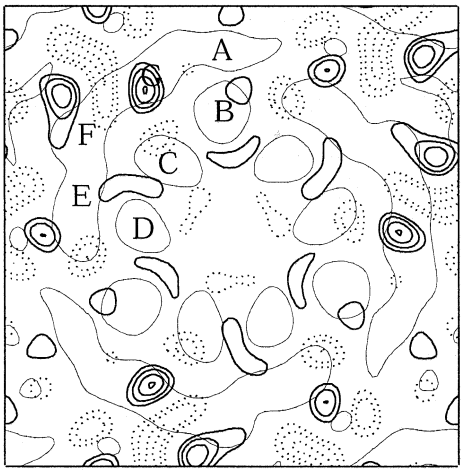

Fig. 6. Two-dimensional difference electron density map of D85N between alkaline and neutral pH. Solid line and dotted line indicate positive and negative density changes, respectively. The outline of the bR molecule is superimposed.

4. Model of the vectorial proton translocation

The results of the structural studies on the photointermediates can be summarized as follows.

(1) Global conformational changes occur during the photoreaction cycle. The large conformational change is corresponding to the M_1 to M_2 transition.

(2) The conformational change occurs in the cytoplasmic half of the molecule. The change brings the opening of the proton channel in the cytoplasmic side.

(3) The conformational change is triggered by the deprotonation of Schiff base.

(4) A subtle but meaningful structural change accompanies the M_2 to N transition.

There is an argument against statement 4 [22]. We suppose that the M-type structure is the transitional structure during the formation process of the N-type structure; the structure should be accumulated during the propagation of the conformational change from the inside to the outside of the proton channel.

We propose a model for the molecular mechanism of the proton pump based on the results (conformation-controlled conformational change model; Fig. 7). We make the following assumptions.

(I) bR can take two conformations, the E conformation and the C conformation. The E and C conformations represent the protein structures whose proton access channel is open to the extracellular and the cytoplasmic side, respectively. There are two sub-states (M_2 and N) in the C conformation.

(II) The E conformation makes the pK_a values of the Schiff base and Asp96 high, while the C conformation lowers both. In other words, the global conformation determines the local environment.

(III) Deprotonation of the Schiff base brings about the E to C conformational change, while reprotonation of the Schiff base causes the C to E conformational change. In other words, the local environmental changes affect the global conformation.

Based on these assumptions, the molecular mechanism of the proton pump is explained as follows. The proton transfer from the Schiff base to Asp85 is induced by photoisomerization of retinal. Deproton-

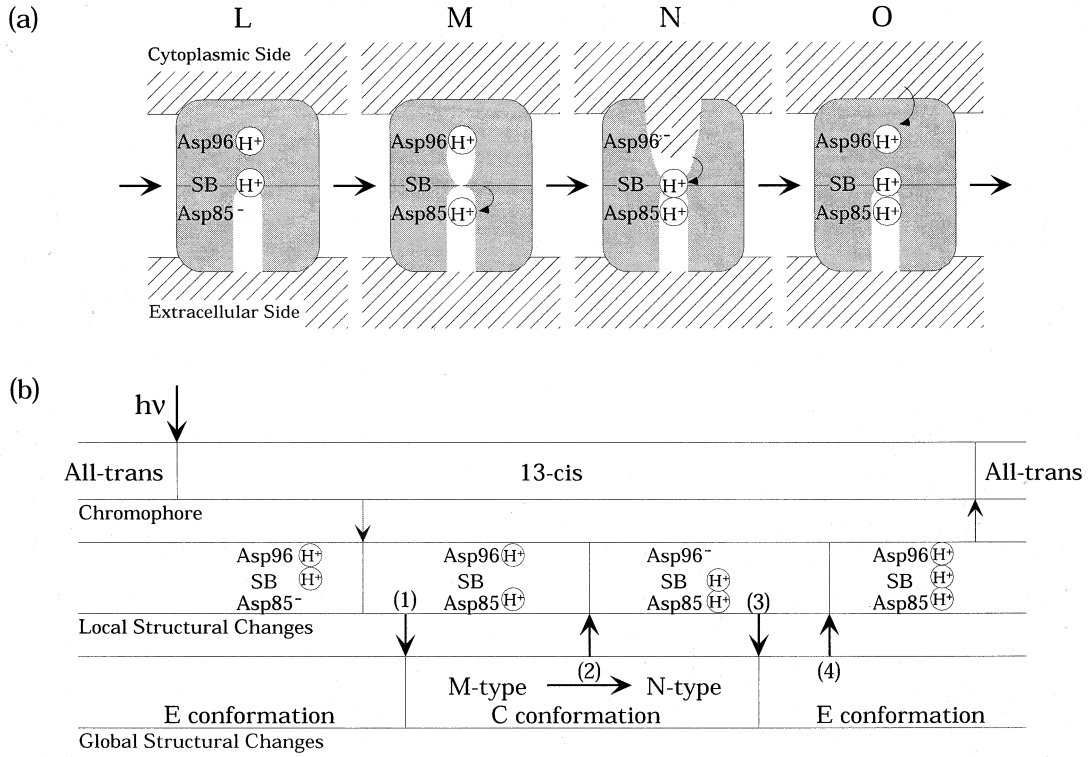

Fig. 7. Model of the proton pump of bacteriorhodopsin. (a) Schematic picture and (b) the relationship between the local proton transfers and tertiary structural changes during photocycle. The vertical bar in each column in (b) indicates the transition from the state shown in the left-hand side to the state in the right-hand side.

ated Schiff base induces the E to C conformational change (process (1) in Fig. 7b). At the M_2 stage, the direct interaction between Asp96 and Schiff base is established, which suppresses the proton release to cytoplasm. Opening of the cytoplasmic channel decreases the pK_a of Asp96, and the proton is transferred to Schiff base (process (2)). Reprotonated Schiff base induces the C to E conformational change (process (3)). The closure of the cytoplasmic channel makes the microenvironment of Asp96 hydrophobic, which causes the reprotonation of Asp96 from the cytoplasm (process (4)), and then the original state is recovered. The essence of this model is that the local chemical reaction such as proton transfer and the global conformational change are closely interrelated as introduced in the assumptions.

Haupt et al. proposed a model with a combination of isomerization, active side switching and ion transfer (IST model) [38]. Isomerization triggers both switch (protein conformational change) and transfer (local reaction) [38]. They supposed that the switch and the transfer are under independent kinetic control [38]. In contrast, the studies on D85N mutant bR had indicated that the deprotonation of the Schiff base and the protein structural change are closely related [20], suggesting that switch and transfer are interrelated. Subramaniam et al. described a similar model, with the assumption that the two conformations are essential components for the proton transport [22]. They also consider that retinal configuration is an important element [22]. They do not refer explicitly to the interrelationship between local reaction and global conformation. We would like to conclude that the close interrelationship between the local reaction and the global conformational change is quite plausible and rational, if we consider the hierarchical protein structure.

During preparation of this review, the crystal structure of the M (MN) intermediate of bR has been solved by X-ray crystal analysis [23]. The structural changes near the G and F helices are clearly observed in the crystal structure. In the future, it is expected that structures to atomic resolution will provide us more precise information about the local changes at each intermediate. However, there are some discrepancies between the crystal structure and the predicted structure based on the low-resolution technique. We should be careful to interpret the structure under physiological conditions and the structure in crystal packing. As shown above, low-resolution techniques provide us with an essence of global conformational changes, which should be explained based on the crystal structure. The knowledge and conceptual model introduced here should be valuable for the better understanding of the proton pump mechanism.

Acknowledgements

The authors would like to express their sincere thanks to Prof. Lanyi (University of California) and Prof. Needleman (Wayne State University) for their fruitful discussions. This work was partly supported by grants from the Ministry of Education, Science, Sports, and Culture of Japan to MK. HK is grateful for the fellowships from the Promotion of Science for Japanese Junior Scientists. Our X-ray diffraction experiments were performed under the approval of the Photon Factory Program Advisory Committee (proposal Nos. 94G077, 96G066 and 99G336).

References

[1] A.E. Blaurock, W. Stoeckenius, Nat. New Biol. 233 (1971) 152–155.
[2] R. Henderson, J.M. Baldwin, T.A. Ceska, F. Zemlin, E. Beckmann, K.H. Downing, J. Mol. Biol. 213 (1990) 899–929.
[3] N. Grigorieff, T.A. Ceska, K.H. Downing, J.M. Baldwin, R. Henderson, J. Mol. Biol. 259 (1996) 393–421.
[4] Y. Kimura, D.G. Vassylyev, A. Miyazawa, A. Kidera, M. Matsushima, K. Mitsuoka, K. Murata, T. Hirai, Y. Fujiyoshi, Nature 389 (1997) 206–211.
[5] K. Mitsuoka, T. Hirai, K. Murata, A. Miyazawa, A. Kidera, Y. Kimura, Y. Fujiyoshi, J. Mol. Biol. 286 (1999) 861–882.
[6] E. Pebay-Peyroula, G. Rummel, J.P. Rosenbusch, E.M. Landau, Science 277 (1997) 1676–1681.
[7] H. Luecke, H.T. Richiter, J.K. Lanyi, Science 280 (1998) 1934–1937.
[8] H. Luecke, B. Schobert, H.T. Richiter, J.P. Cartailler, J.K. Lanyi, J. Mol. Biol. 291 (1999) 899–911.
[9] H.G. Khorana, J. Biol. Chem. 263 (1988) 7439–7442.
[10] R.A. Mathies, S.W. Lin, J.B. Ames, W.T. Pollard, Annu. Rev. Biophys. Biophys. Chem. 20 (1991) 491–518.
[11] J.K. Lanyi, Biochim. Biophys. Acta 1183 (1993) 241–261.

[12] N.A. Dencher, D. Dresselhaus, G. Zaccai, G. Büldt, Proc. Natl. Acad. Sci. USA 86 (1989) 7876–7879.
[13] M.H.J. Koch, N.A. Dencher, D. Oesterhelt, H.-J. Plöhn, G. Rapp, G. Büldt, EMBO J. 10 (1991) 521–526.
[14] M. Nakasako, M. Kataoka, Y. Amemiya, F. Tokunaga, FEBS Lett. 292 (1991) 73–75.
[15] S. Subramaniam, M. Gerstein, D. Oesterhelt, R. Henderson, EMBO J. 12 (1993) 1–8.
[16] H. Kamikubo, M. Kataoka, G. Váró, T. Oka, F. Tokunaga, R. Needleman, J.K. Lanyi, Proc. Natl. Acad. Sci. USA 93 (1996) 1386–1390.
[17] J. Vonck, Biochemistry 35 (1996) 5870–5878.
[18] J.K. Lanyi, G. Váró, Isr. J. Chem. 35 (1995) 365–385.
[19] J.K. Lanyi, J. Biol. Chem. 272 (1997) 31209–31212.
[20] M. Kataoka, H. Kamikubo, F. Tokunaga, L.S. Brown, Y. Yamazaki, A. Maeda, M. Sheves, R. Needleman, J.K. Lanyi, J. Mol. Biol. 243 (1994) 621–638.
[21] J.K. Lanyi, Nature 375 (1995) 461–463.
[22] S. Subramaniam, M. Lindahl, P. Bullough, A.R. Faruqi, J. Tittor, D. Oesterhelt, L. Brown, J. Lanyi, R. Henderson, J. Mol. Biol. 287 (1999) 145–161.
[23] H. Luecke, B. Schobert, H.T. Richiter, J.P. Cartailler, J.K. Lanyi, Science 286 (1999) 255–261.
[24] R.M. Glaser, J.M. Baldwin, T.A. Ceska, R. Henderson, Biophys. J. 50 (1986) 913–920.
[25] H.J. Sass, I.W. Schachowa, G. Rapp, M.H.J. Koch, D. Oesterhelt, N.A. Dencher, G. Büldt, EMBO J. 16 (1997) 1484–1491.
[26] M. Ferrand, A.J. Dianoux, W. Petry, G. Zaccai, Proc. Natl. Acad. Sci. USA 90 (1993) 9668–9672.
[27] M. Kataoka, H. Kamikubo, J. Yunoki, F. Tokunaga, T. Kanaya, Y. Izumi, K. Shibata, J. Phys. Chem. Solids 60 (1999) 1285–1289.
[28] G. Zaccai, J. Mol. Biol. 194 (1987) 569–572.
[29] M. Nakasako, M. Kataoka, F. Tokunaga, FEBS Lett. 254 (1989) 211–214.
[30] J. Sasaki, Y. Shichida, J.K. Lanyi, A. Maeda, J. Biol. Chem. 267 (1992) 20782–20786.
[31] T. Oka, H. Kamikubo, F. Tokunaga, J.K. Lanyi, R. Needleman, M. Kataoka, Photochem. Photobiol. 66 (1997) 768–773.
[32] T. Oka, H. Kamikubo, F. Tokunaga, J.K. Lanyi, R. Needleman, M. Kataoka, Biophys. J. 76 (1999) 1018–1023.
[33] H. Kamikubo, T. Oka, Y. Imamoto, F. Tokunaga, J.K. Lanyi, M. Kataoka, Biochemistry 36 (1997) 12282–12287.
[34] T. Oka, Ph.D. thesis, Graduate School of Science, Osaka University, Osaka, 2000.
[35] O. Jardetzky, Nature 211 (1966) 969–970.
[36] G.J. Turner, L.J.W. Miercke, T.E. Thorgeirsson, D.S. Kliger, M.C. Betlach, R.M. Stroud, Biochemistry 32 (1993) 1332–1337.
[37] L.S. Brown, H. Kamikubo, L. Zimányi, M. Kataoka, F. Tokunaga, P. Verdegem, J. Lugtenburg, J.K. Lanyi, Proc. Natl. Acad. Sci. USA 94 (1997) 5040–5044.
[38] U. Haupts, J. Tittor, E. Bamberg, D. Oesterhelt, Biochemistry 36 (1997) 2–7.
[39] P.J. Kraulis, J. Appl. Crystallogr. 24 (1991) 946–950.